Microstructural evolution of a Ti-4.5Al-3Mo-1V alloy during hot working

Y. Y. ZONG*, D. B. SHAN, Y. LU
Department of Materials Science and Engineering, Harbin Institute of Technology, Harbin, 150001, People's Republic of China
E-mail: hagongda@hit.edu.cn

Published online: 10 April 2006

The study investigated the variation of microstructure of a Ti-4.5AL-3Mo-1V alloy during hot compressing in $\alpha + \beta$ phase field. By scanning electron microscopy (SEM) and transmission electron microscopy (TEM), we systematically examined the influences of hot working parameters on the microstructural features including of the morphology of α grain, volume fraction of α phase and dynamic recrystallization (DRX). The experimental evidence showed that both α and β phases underwent DRX under the experimental conditions. Moreover, the recrystallization degree of α phase was more sufficient than that of β phase. The DRX was accelerated with increase of deformation temperature and decrease of strain rate. It was also noted that a certain degree of the ($\alpha \rightarrow \beta$) phase transformation occurred concurrently with the mechanical deformation. In accordance with the microstructural evolution, flow curves of the alloy were characterized by a linear increase until regular oscillations at high strain rates or single peak at low strain rates and softening was followed.
© *2006 Springer Science + Business Media, Inc.*

1. Introduction

Due to the specific strength, excellent fracture toughness, extensive ductility and good corrosion resistance titanium alloys, especially for $\alpha + \beta$ alloys, are widely used in aerospace, marine and biomedicine. Moreover, they must be used more efficiently if they are to meet the performance demands of this century [1–3]. The Russian Ti-4.5AL-3Mo-1V (BT14) alloy is a typical $\alpha + \beta$ alloy and is widely used in rockets. Since bulk forming is often performed under compression loading conditions, there are many investigations carried out on the hot compression behavior of many $\alpha + \beta$ titanium alloys [4–8]. However, the Russian alloy Ti-4.5AL-3Mo-1V is less commonly known and no open report has been found on its hot deformation behavior. It is widely accepted that mechanical properties of alloys are very sensitive to the characteristics of the microstructure. For titanium alloys, flow stress behavior and microstructural evolution during plastic deformation are, to a great extent, determined by temperature as well as strain rate [9–11].

For a clearer understanding and control of the correlation between processing and microstructure and properties of Ti-4.5AL-3Mo-1V alloy, the objective of this work is to investigate the variation of its microstructure under different hot working conditions using SEM and TEM. This work will also point out the influence of the hot working parameters, such as deformation temperature and strain rate, on the flow stress behavior and microstructural features of Ti-4.5AL-3Mo-1V alloy, especially on the type of phase present, the morphologies of the α phase, grain size and shape, the $\alpha \rightarrow \beta$ phase transformation and DRX.

2. Experimental methods and procedures

2.1. Materials and specimen preparation

A 2.5 mm thick Ti-4.5AL-3Mo-1V sheet was used in this study. The β transus reported for this material is approximately 940°C. Its chemical composition is presented in Table I and its microstructure is shown in Fig. 1. As seen from Fig. 1, the microstructure of the alloy was mainly characterized by reciprocally parallel lamellar α phase and β phase. The bright phase represents α and the dark phase is β. There was no Ti-4.5AL-3Mo-1V alloy bar at that time. In order to study the hot forging behavior of the alloy, a plate of 10.5 mm thickness was obtained by adhering four 2.5 mm thick sheets together with silver conductive adhesive. Cylin-

*Author to whom all correspondence should be addressed.

0022-2461 © *2006 Springer Science + Business Media, Inc.*
DOI: 10.1007/s10853-006-2658-z

TABLE I Chemical composition of Ti-4.5AL-3Mo-1V alloy (wt.%)

Al	Mo	V	C	Fe	Si	Zr	O	N	Ti
3.5–6.3	2.5–3.8	0.9–1.9	0.10	0.25	0.15	0.30	0.15	0.05	balanc

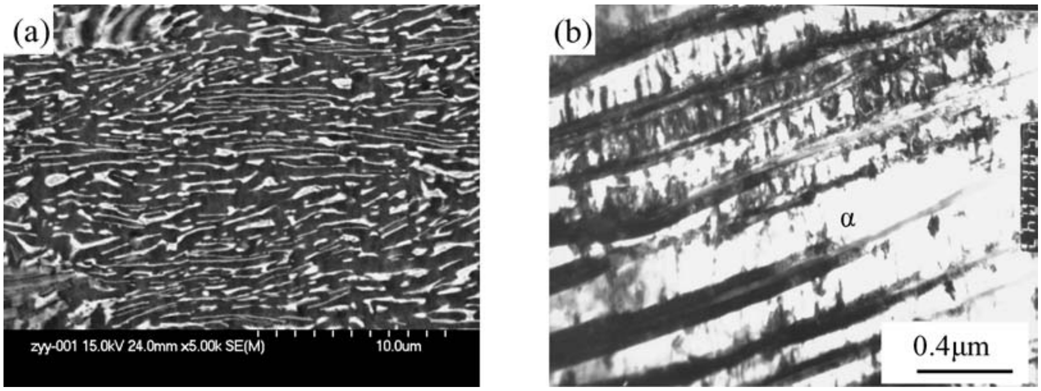

Figure 1 Initial microstructure of experimental materials: (a) SEM microstructure and (b) TEM microstructure.

drical compression specimens of 7 mm diameter and 10.5 mm height were machined from the plate.

2.2. Hot compression

Isothermal hot compression tests were carried out on a Gleeble-1500 simulator. Experiments were conducted in $\alpha + \beta$ phase field at deformation temperatures of 600, 650, 700, 750 and 800°C and strain rates of 0.01, 0.1, 1.0 and 10 s^{-1}. The high reduction of all the specimens was 60%. The specimens were resistance heated by thermocouples feedback. The specimens were heated to compression temperature at a heating rate of 5°C/s and homogenized for 300 s before deformation. After hot compression, the specimens were quenched immediately in water. Deformed specimens are shown in Fig. 2. For studying the influence of deformation on the microstructure, five additional samples were heated to different temperatures respectively, and then quenched in water without deformation.

2.3. Microstructure tests

The deformed specimens were axially sectioned parallel to the compression axis and the cut surface was prepared for SEM examination using standard polishing and etching techniques. Information about deformation inhomogeneities was derived from observations by SEM images at sites A, B, C and D of the specimen deformed at 600°C and strain rate of 1 s^{-1}. All of the other SEM images were observed at site C (Fig. 2b). A thick film was transversely sectioned on either of the middle two sheets and then prepared for thin foil specimens for observation in TEM. The area content and the mean grain size of alpha phase are measured by the quantitative metallographic image analysis system.

3. Results and discussion

3.1. Flow stress behavior

The typical true stress-true strain curves of the Ti-4.5Al-3Mo-1V alloy exhibit some characteristic shapes as shown in Fig. 3. The equation $\bar{\sigma} = \sigma_0(1 + 2mr/3\sqrt{3}h)$ is used to correct the discrepancy between measured stress $\bar{\sigma}$\$ and true stress σ_0 caused by friction. Here m is the friction coefficient, r and h are the transient radius and height of the specimen respectively.

In general, when a stress strain curve displays a stress peak after yielding and then following with a gradual de-

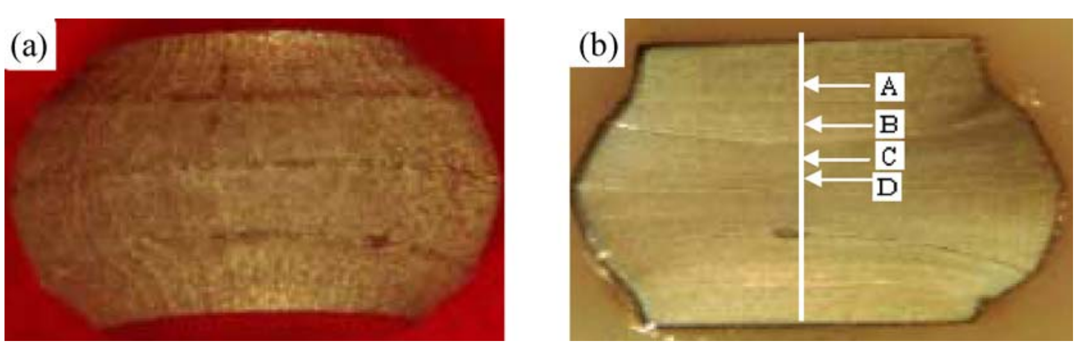

Figure 2 Compressed specimen: (a) external appearance and (b) section appearance.

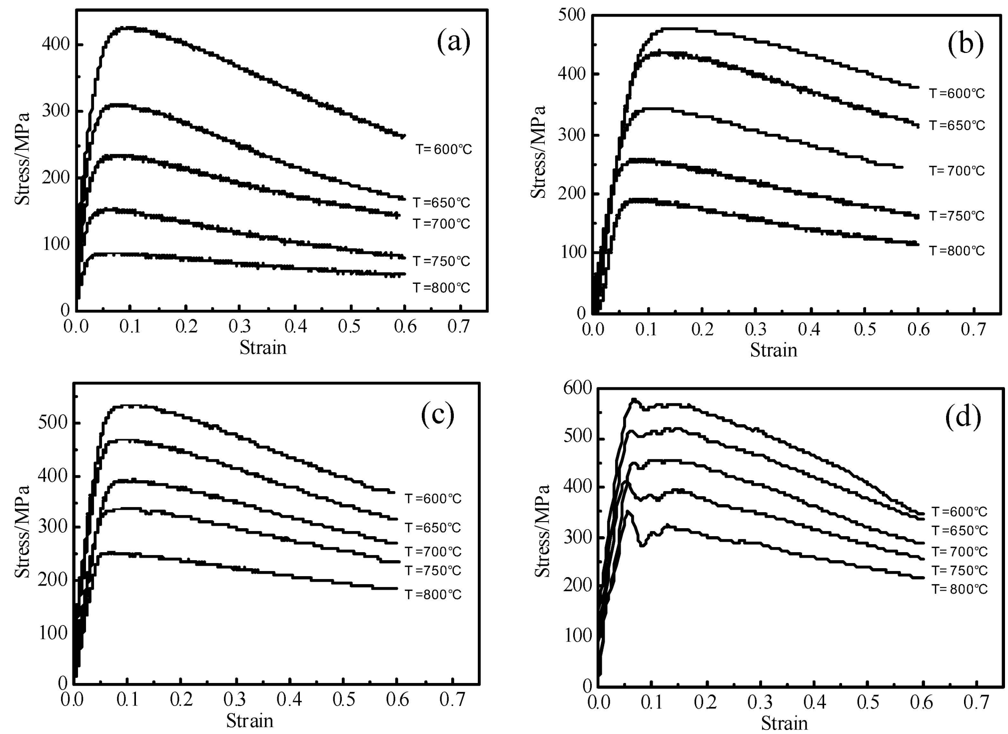

Figure 3 True stress-strain curves of the Ti-4.5AL-3Mo-1V alloy compressed at different parameters: (a) 0.01 s^{-1}, (b) 0.1 s^{-1}, (c) 1 s^{-1} and (d) 10 s^{-1}.

crease of stress, this indicates that DRX has taken place [12]. As shown in Fig. 3, all curves of the Ti-4.5Al-3Mo-1V alloy exhibit this characteristic shape. Corresponding to the behavior, the softening mechanism of the Ti-4.5Al-3Mo-1V during hot compressing in the two-phase field is DRX, which is confirmed by the microstructure as will be discussed later. At low strain rates, the flow stress curves are characterized by a linear increase until a peak after which flow softening is observed. At high strain rates, typically 10 s^{-1}, multiple stress peaks are followed by a rapid decrease of stress. Taku Sakai [13] discussed the changeover from multiple to single peak behavior of flow curves under the condition of DRX by the relative grain size (D_0/D_s), where D_o and D_s are the initial and stable dynamic grain sizes. The flow stress is sensitive to temperature and strain rate and steeply falls with increasing temperature and decreasing strain rate. The softening mechanism of the Ti-4.5AL-3Mo-1V alloy is mainly DRX. Except for the effects of temperature and strain rate, this softening phenomenon may be also attributed to two other reasons: adiabatic heating which raises the actual temperature of the specimen and the increasing proportion of the soft β phase during deformation.

3.2. Structure observation

Microstructures of the specimens heated to the five temperatures and without deformation are shown in Fig. 4. It is seen that the α-lamellae gradually transform into numerous small spherical grains with increasing heating temperature through melting and globurizing. The melting site is shown in Fig. 4a. When heating temperature is up to 800°C, most of the α-lamellae are melted into granular α grains whose shapes and sizes may be different. Meanwhile, more energy is stored for the phase transformation with the increase of heating temperature, which leads to more diffusion and decrease of volume fraction of α phase.

The parent α grain size, the α volume fraction and the α grain pattern pose a great effect on the mechanical properties of $\alpha + \beta$ titanium alloys [14,15]. SEM images of the Ti-4.5Al-3Mo-1V alloy hot compressed at different conditions are presented in Figs. 5 and 6. It can be seen that parent α phase is plastically deformed during hot working in the $(\alpha + \beta)$ phase field. At relatively high deformation temperatures, a low volume fraction of α phase is present during deformation due to phase transformation. According to their initial orientations, some of the α grains are distorted and others are fibrous.

Figs. 7 and 8 show representative micrographs of α phase with different DRX degrees during hot working in the two-phase field. Former experiments showed that DRX was an important phenomenon that could occur in the hot working of two-phase titanium alloys [8, 16]. L.X. Li *et al*. [8] observed that for the Ti-3Al-5V-5Mo (BT16) alloy deformed in $\alpha + \beta$ phase region (700–860°C) and strain rate region of 0.05–15s^{-1}, only α phase underwent DRX. R.Ding *et al*. [17] reported that DRX was not involved in the Ti-6Al-4V (TC4) alloy during hot working in the $(\alpha + \beta)$ phase field (850–995°C) and strain rate region of 0–1 s^{-1}.This experimental evidence shows that DRX occurs during hot working of the Ti-4.5Al-3Mo-1V alloy. As can be seen from Fig. 8c, both α phase and β phase undergoes DRX, which is different from BT16 and TC4

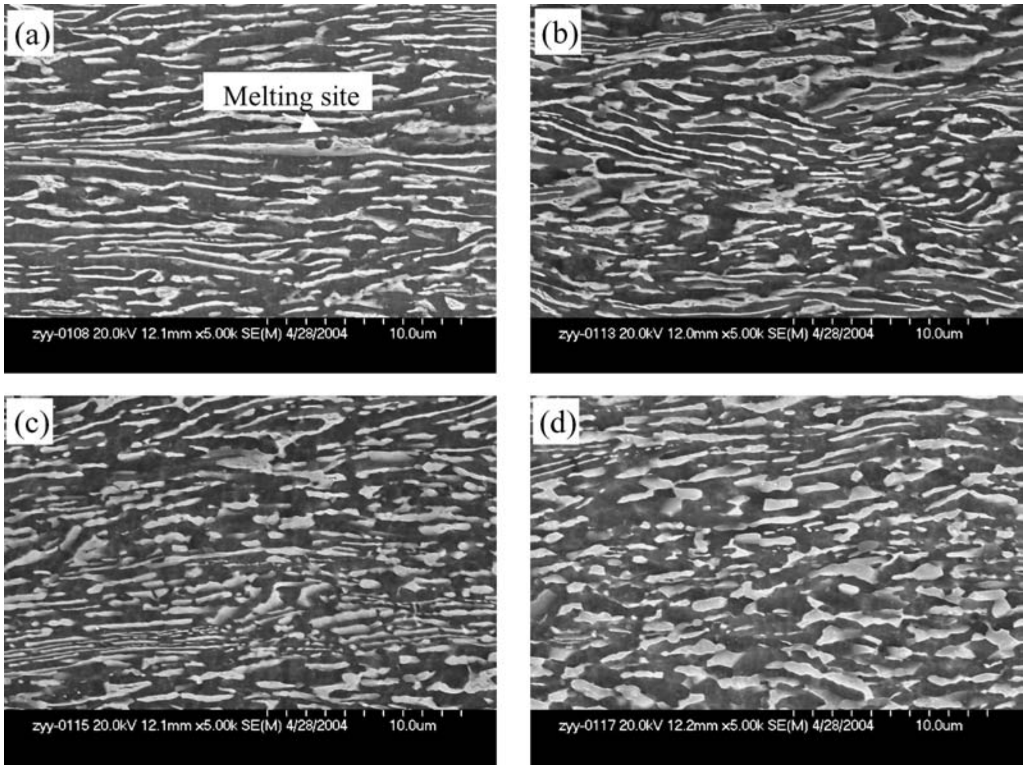

Figure 4 SEM images of the specimens without deformation: (a) 600°C, (b) 700°C, (c) 750°C and (d) 800°C.

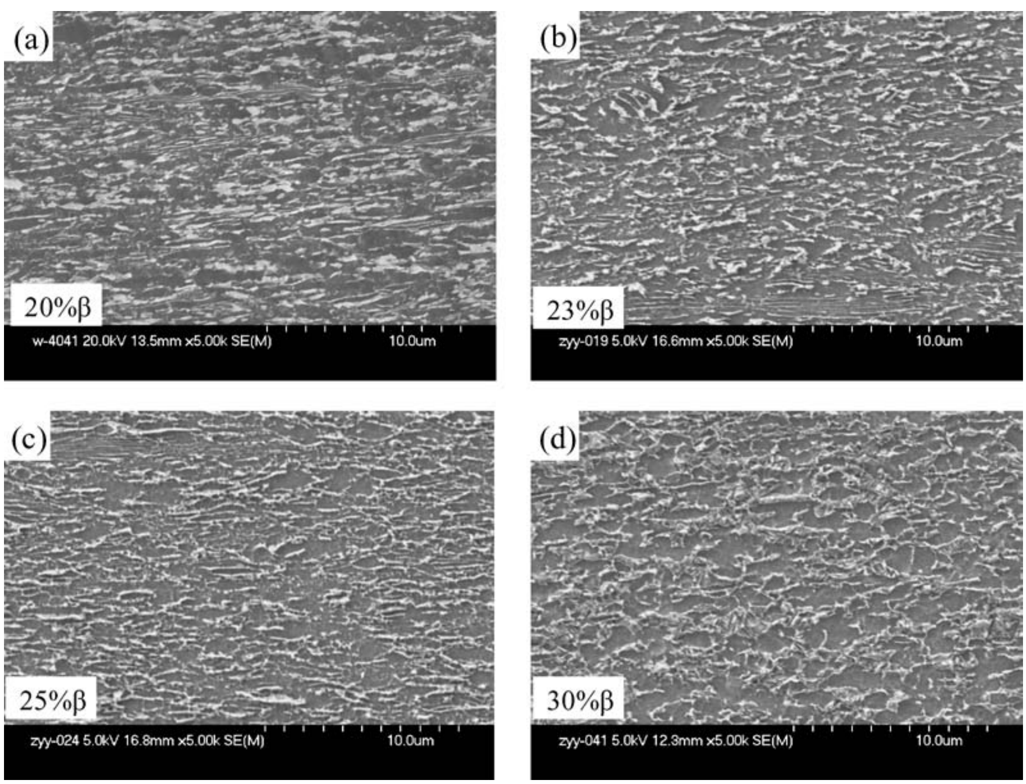

Figure 5 SEM images of the Ti-4.5AL-3Mo-1V alloy compressed at 0.1 s^{-1}: (a) 650°C, (b) 700°C, (c) 750°C and (d) 800°C.

alloy. Further, dynamic nucleation occurs mainly inside α-lamella and at the phase boundaries. It can also be seen that under the same deformation conditions, DRX preferentially occurs in the α phase and that DRX velocity of α phase is faster than that of β phase. Li Miaoquan [16] also suggested that when a two-phase titanium alloy is deformed at a given temperature, the recrystallization velocity of α phase is faster than that of β phase. In the case of high temperatures and very low strain rates, DRX also occurs in the β phase, as shown in Fig. 8c. This is due to

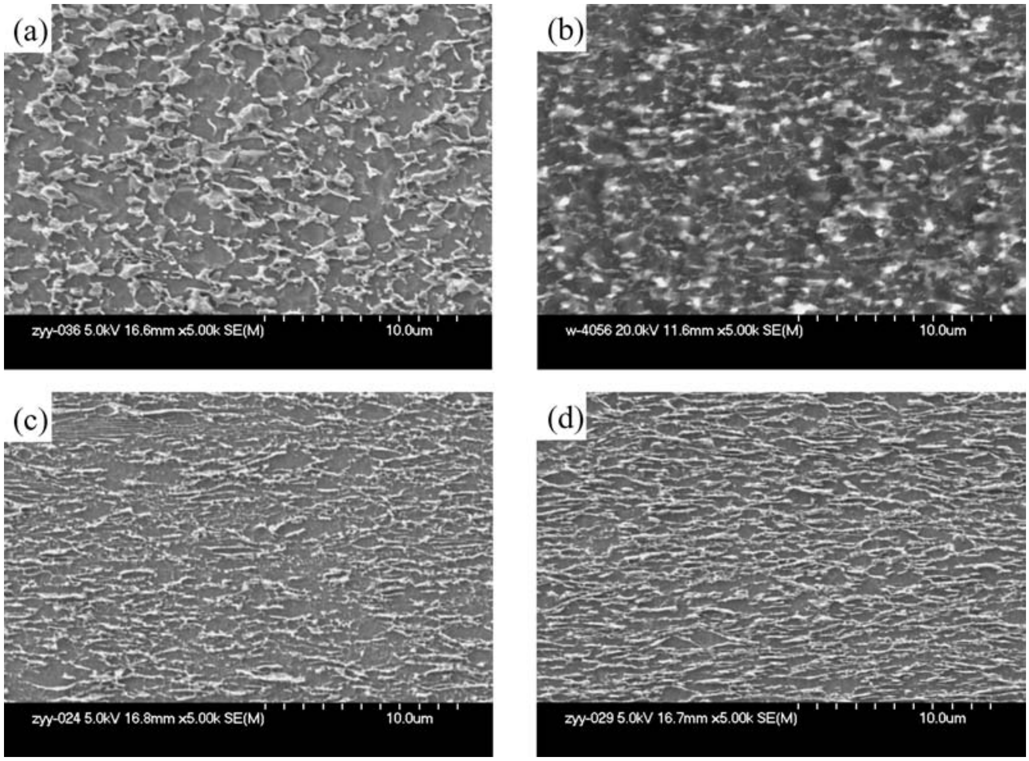

Figure 6 SEM images of the Ti-4.5AL-3Mo-1V alloy compressed at 750°C: (a) 0.01 s^{-1}, (b) 0.1 s^{-1}, (c) 1 s^{-1} and (d) 10 s^{-1}.

the difficulty of obtaining DRX in the bcc β phase. In addition, many equiaxed α grains surround one β DRX grain.

3.2.1. Effect of strain

By comparing the microstructures of Figs. 4–6, it can be seen that deformation causes a grain refinement of the α phase. This may be attributed to the fact that fragmentation degree of grains and DRX degree both increase with the hot plastic deformation. In addition, the volume fraction of α phase decreases with the deformation. This is because a certain degree of the ($\alpha \rightarrow \beta$) phase transformation occurs concurrently with the mechanical deformation. Due to DRX and high volume fraction of soft β phase, flow stress decreases with the increase of strain, as shown in Fig. 3. Deformation inhomogeneity caused by friction between specimen surface and die is noticeable in one deformed specimen. The actual deformation degree in the central region of the specimen is higher than that in the surface zones (Fig. 2). The inhomogeneous microstructure of a deformed specimen is presented in Fig. 9. The spheroidization degree of α grains is described by the formula d/l, where d and l are α grain length (l) and width (d) respectively. The effect of strain on the morphology of α grain is shown in Table II. It can be seen that the larger the deformation degree the finer the microstructure is, and the more obvious spheroidization of αgrains is. This is because sufficient deformation is the impetus for DRX. The energy storage increases with the increase of deformation degree, so DRX is more likely to come into being.

3.2.2. Effect of temperature

As shown in Fig. 7, when other deformation parameters are the same, the higher the temperature, the more DRX grains occur in the deformed specimens. But temperature has little influence on the DRX grain size. The increase of the amount of exquiaxed DRX grains indicates the increase of DRX degree. The DRX degree is relatively small at low temperatures. This is because diffusion increases with the increase of temperature and thus DRX occurs more easily. Due to the influence of the DRX, the globularization of α phase increases with increasing temperature, which is shown in Fig. 5. Correspondingly, flow stress decreases with the increase of temperature, as shown in Fig. 10a. The static starting and ending recrystallization temperatures of Ti-4.5Al-3Mo-1V are 900°C and 930°C respectively. However, as can be seen from Fig. 7a, DRX of α phase has occurred when the temperature is 600°C. This may be due to the following reasons: adiabatic heating, poor thermal conductivity of the titanium alloy and the deformation inhomogeneities. These three all lead to higher actual temperatures in the central region. As a result, the flow stress compressed at 600°C tends to gradually decline after the maximum (Fig. 3), which indicates that DRX occurs in the specimens deformed at 600°C.

3.2.3. Effect of strain rate

In the past, some researchers analyzed the influence of deformation rate on the mechanism of $\beta \rightarrow \alpha + \beta$ transformation, which in turn influenced the morphology of

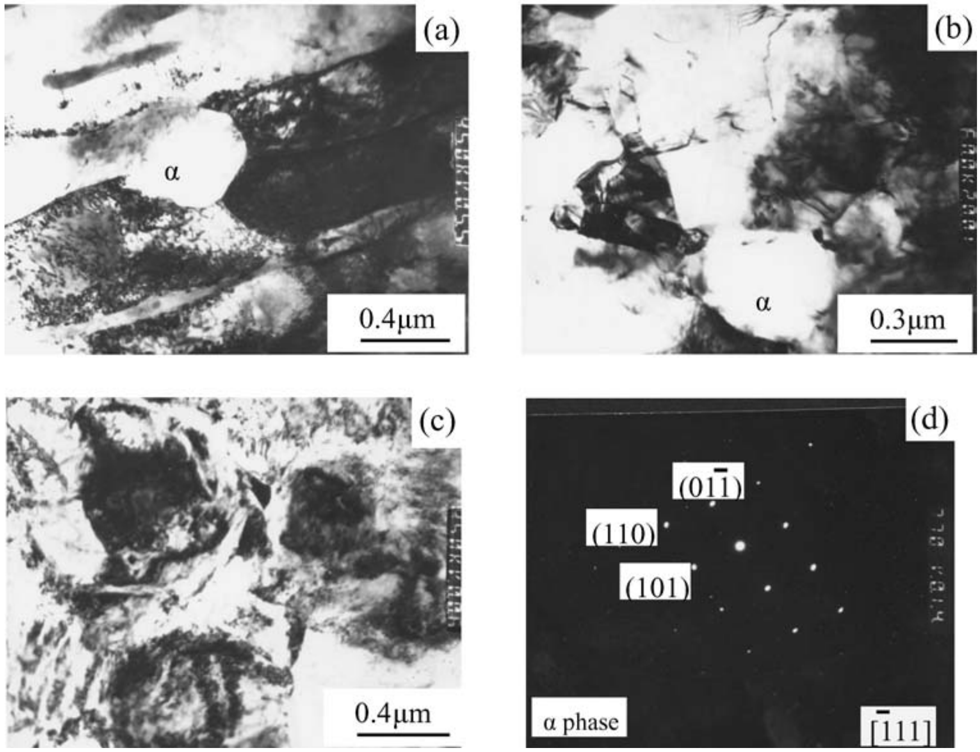

Figure 7 TEM images of the Ti-4.5AL-3Mo-1V alloy compressed at 0.1 s^{-1}: (a) 600°C, (b) 700°C and (c) 800°C (d) selected area diffraction patterns of α phase.

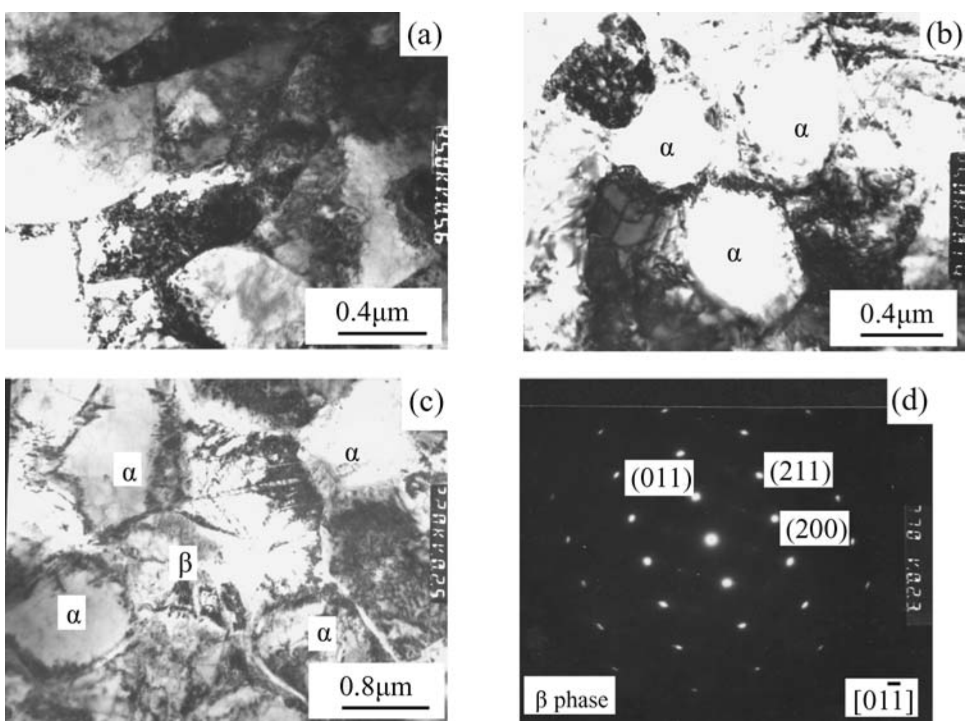

Figure 8 TEM images of the Ti-4.5AL-3Mo-1V alloy compressed at 800°C: (a) 1 s^{-1}, (b) 0.1 s^{-1} and (c) 0.01 s^{-1}, (d) selected area diffraction patterns of β phase.

the α phase [18]. In this study, attempts have been made toward understanding the effect of strain rate on the DRX and its significant changes in the morphology of both phases. Taku Sakai [13] classified the DRX grains into three categories: (i) DRX nuclei, (ii) growing DRX grains containing a dislocation density gradient, and (iii) critically work hardened DRX grains which contain fairly homogeneous and more clearly developed substructures. DRX is a dynamic process. When DRX is very sufficient, high-density dislocations occur at boundaries and inside

TABLE II Effect of strain on the morphology of α grain (600°C, 1 s^{-1})

Location	ε	Mean grain size of α grain	α grain shape (d/l)
A	0.2	0.96 μm	0.05–0.2
B	0.4	0.90 μm	0.1–0.3
C	0.6	0.76 μm	0.2–0.5
D	0.8	0.57 μm	0.5–0.8

TABLE III Effect of strain rate on the DRX grain size (800°C)

Strain rate	0.01 s^{-1}	0.1 s^{-1}	1 s^{-1}
DRX α grain size	1 μm	0.6 μm	0.4 μm
DRX β grain size	2 μm	none	none

DRX grains because of the deformation after DRX. As shown in Fig. 8, the three types of DRX grains occur in the specimens at different strain rates. When strain rate is 1 s^{-1}, only dynamic nucleus occur, creating grains in the first category. When strain rate is 0.1 s^{-1}, many critically work hardened DRX grains are formed, resulting in the second category of grains. High-density dislocations at the boundaries of the DRX grains can be seen clearly after the DRX grains are pressed. The DRX grains formed at 0.01 s^{-1} belong to the third category. The original lamellar structure is changed completely to equiaxed DRX grains. Results clearly indicate that the degree of DRX increases with the decrease of strain rate. In addition, strain rate has great influence on the DRX grain size, as shown in Table III. It can be seen that the equiaxed grain size increases with the decrease of strain rate. This

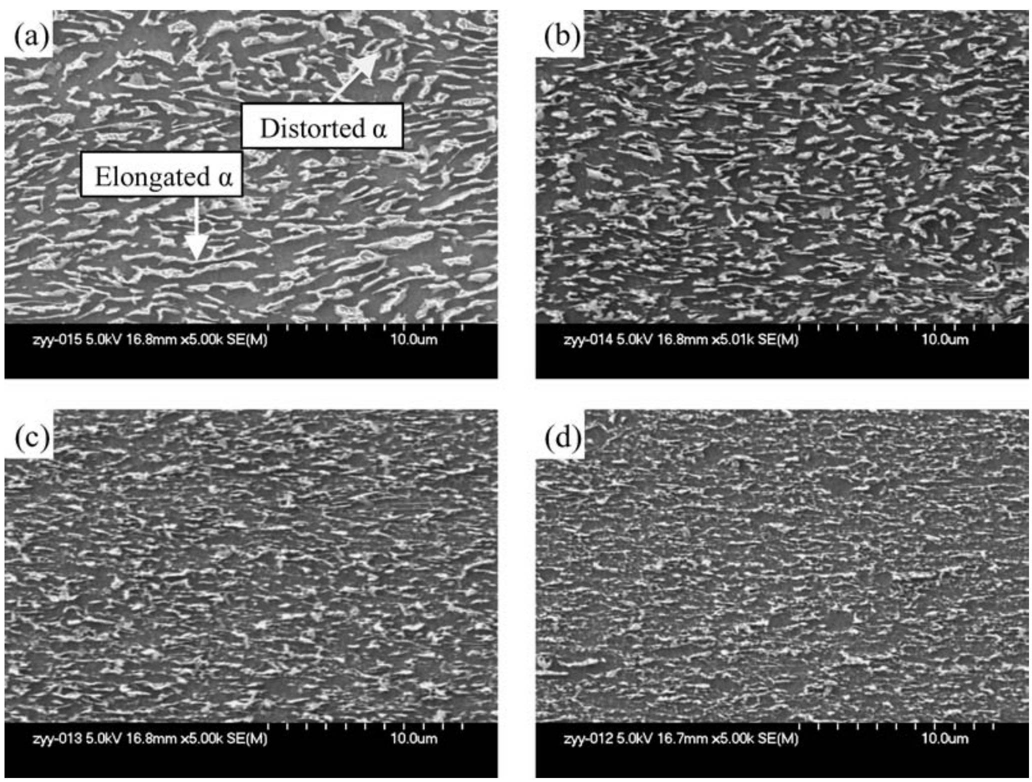

Figure 9 Microstructures of (a) site A, (b) site B, (c) site C and (d) site D in the deformed specimen hot compressed at 600°C and 1 s^{-1}.

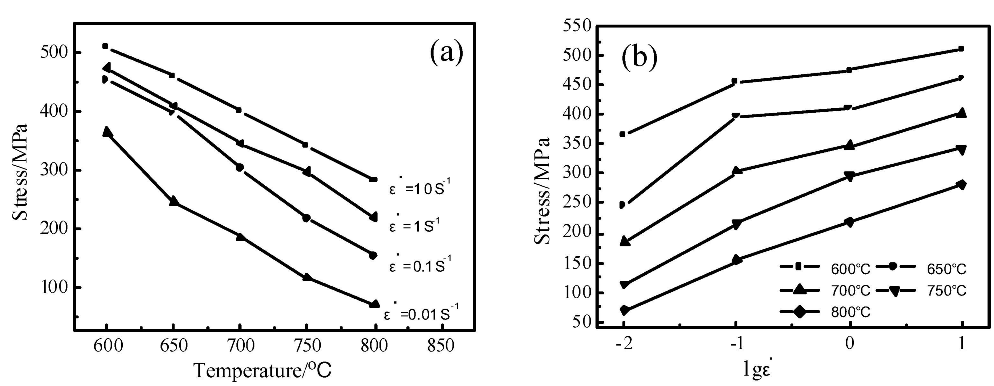

Figure 10 Variation of flow stress with (a) strain rate at different temperatures and (b) temperature at different strain rates at a strain of 0.3

is because DRX (involving nucleation and grain growth) needs time. When the strain rate is relatively low, the DRX grain has more time to nucleate and grow. At high strain rates, the accumulated energy increases, as dislocations have not enough time to consume or continually generate. The presence of excess dislocations can lead to heterogeneous nucleation of both phases on dislocations. However, the diffusion cannot proceed completely and DRX grain growth is not so pronounced because of the very short deformation time. Therefore, as shown in Fig. 6, an increase of strain rate is found to cause a grain refinement of the α phase. In accordance with the microstructural evolution, the flow stress increases with the increase of strain rate, as shown in Fig. 10b. These microstructural observations indicate that strain rate causes a significant change in the DRX leading to a change in the morphology of the α phase.

In conclusion, deformation temperature and strain rate causes tremendous changes in the microstructural evolution, which in turn influences the behavior of flow stress. The influence of temperature and strain rate on the flow stress is in accordance with the microstructural evolution (shown in Fig. 10).

4. Conclusion

The deformation behavior of the Ti-4.5AL-3Mo-1V alloy has been determined by hot compression tests over a practical range of temperatures and strain-rates. The results can be summarized as follows:

1. The spheroidization of lamellar α phase in the specimens without deformation increases with the temperature due to diffusional process. Severe hot plastic deformation contributes to phase transformation and grain refinement due to DRX.
2. Due to the influence of the adiabatic heating, poor thermal conductivity of the titanium alloy and deformation inhomogeneties of specimens, DRX occurs in the Ti-4.5AL-3Mo-1V alloy at 600°C.The increase of temperature causes an increase of DRX degree, but has little influence on the DRX grain size.
3. Strain rate causes significant changes to the DRX of α phase, which in turn influences the morphology of α phase in the Ti-4.5AL-3Mo-1V alloy during compressing in the two-phase field. The DRX grain size increases with decreasing strain rate. The higher the strain rates the finer the microstructure.
4. DRX is an important feature of the Ti-4.5AL-3Mo-1V alloy hot compressed in the two-phase field. Both α and β phases undergo DRX under the experimental conditions. At the same deformation conditions, DRX preferentially occurs in the α phase.
5. In accordance with the microstructural evolution, flow curves of the Ti-4.5AL-3Mo-1V alloy are characterized by a linear increase until regular oscillations at high strain rates or single peak at low strain rates after which flow softening is observed. The flow stress decreases with increasing temperature and decreasing strain rate.

Acknowledgements

The authors are extremely grateful to Dr. Wenchen Xu for his enthusiasm and help with this study and extend thanks to Processor Qingchang Meng for his valuable assistance in TEM examination.

References

1. MITSUO NIINOMI, *Sci. Tech. Adv. Mater.* **4** (2003) 445.
2. D. M. GORDIN, T. GLORIANT, G. TEXIER and I. THIBON, *J. Mater. Sci.* **15** (2004) 885.
3. W. J. EVANS, *Mater. Sci. Eng.* **A243** (1998) 89.
4. JI ZHANG and ZHIHONG ZHANG, *Intermetallics.* **8** (2000) 321.
5. L. X. LI and Y. LOU, *Mater and Design.* **20** (2002) 451.
6. R. M. MILLER and T. R. BIELER, *Scripta Mater.* **40** (1999) 1387.
7. C. HUANG and JOSEPH K. L. LAI, *J. Mater. Proce. Tech.* **73** (1998) 119.
8. G. LÜ TJERING, *Mater. Sci. Eng.* **A243** (1998) 32.
9. GUOXIN CAO and LIANFENG FU, *Intermetallics.* **8** (2000) 647.
10. F. PERDRIX and M. F. TRICHET, *ibid.* **9** (2001) 807.
11. DIRK OSTWALDT and PETER KLIMANEK, *Mater. Sci. Eng.* **A234–236** (1997) 810.
12. T. TAKASUGI and Y. WATANABE, *Scripta Mater.*. **43** (2000) 485.
13. TAKU SAKAI, *J. Mater. Proc. Tech.*, **53** (1995) 349.
14. R. FILIP and K. KUBIAK, *ibid.* **133** (2003) 84.
15. S. L. SEMIATIN and T. R. BIELER, *Acta Mater.* **49** (2001) 3565.
16. LI MIAOQUAN and XIONG AIMING, *Mater. Charact.* **49** (2003) 203.
17. R. DING and Z. X. GUO, *Mater. Sci. Eng.* **A365** (2004) 172.
18. T. SESHACHARYULU and B. DUTTA, *Scripta Mater.* **46** (2002) 673.

Received 19 March
and accepted 31 May 2005